

## Excited-State Aromatic Interactions in the Aggregation-Induced Emission of Molecular Rotors

Jiri Sturala, Marc K. Etherington, Aisha N Bismillah, Heather F. Higginbotham, William John Trewby, Juan A Aguilar, Elizabeth H. C. Bromley, Alyssa-Jennifer Avestro, Andrew P. Monkman, and Paul R. McGonigal

*J. Am. Chem. Soc.*, **Just Accepted Manuscript** • Publication Date (Web): 18 Nov 2017

Downloaded from <http://pubs.acs.org> on November 18, 2017

### Just Accepted

“Just Accepted” manuscripts have been peer-reviewed and accepted for publication. They are posted online prior to technical editing, formatting for publication and author proofing. The American Chemical Society provides “Just Accepted” as a free service to the research community to expedite the dissemination of scientific material as soon as possible after acceptance. “Just Accepted” manuscripts appear in full in PDF format accompanied by an HTML abstract. “Just Accepted” manuscripts have been fully peer reviewed, but should not be considered the official version of record. They are accessible to all readers and citable by the Digital Object Identifier (DOI®). “Just Accepted” is an optional service offered to authors. Therefore, the “Just Accepted” Web site may not include all articles that will be published in the journal. After a manuscript is technically edited and formatted, it will be removed from the “Just Accepted” Web site and published as an ASAP article. Note that technical editing may introduce minor changes to the manuscript text and/or graphics which could affect content, and all legal disclaimers and ethical guidelines that apply to the journal pertain. ACS cannot be held responsible for errors or consequences arising from the use of information contained in these “Just Accepted” manuscripts.

# Excited-State Aromatic Interactions in the Aggregation-Induced Emission of Molecular Rotors

Jiri Sturala,<sup>†,‡</sup> Marc K. Etherington,<sup>‡</sup> Aisha N. Bismillah,<sup>†</sup> Heather F. Higginbotham,<sup>‡</sup> William Trewby,<sup>‡</sup> Juan A. Aguilar,<sup>†</sup> Elizabeth H. C. Bromley,<sup>‡</sup> Alyssa-Jennifer Avestro,<sup>\*,†</sup> Andrew P. Monkman<sup>\*,†</sup> and Paul R. McGonigal<sup>\*,†</sup>

<sup>†</sup>Department of Chemistry and <sup>‡</sup>Department of Physics, Durham University, Lower Mountjoy, Stockton Road, Durham, DH1 3LE, United Kingdom

**KEYWORDS** *Molecular Rotors, Aggregation-Induced Emission, Fluorescence, Aromatic Interactions, Carbocycles*

**ABSTRACT:** Small, apolar aromatic groups, such as phenyl rings, are commonly included in the structures of fluorophores in order to impart hindered intramolecular rotations, leading to desirable solid-state luminescence properties. However, they are not normally considered to take part in through-space interactions that influence the fluorescent output. Here, we report on the photoluminescence properties of a series of phenyl-ring molecular rotors bearing three, five, six, and seven phenyl groups. The fluorescent emissions from two of the rotors are found to originate, not from the localized excited state as one might expect, but from unanticipated through-space aromatic dimer states. We demonstrate that these relaxed dimer states can form as a result of intra- or intermolecular interactions across a range of environments in solution and solid samples, including conditions that promote aggregation-induced emission. Computational modeling also suggests that the formation of aromatic-dimer excited states may account for the photophysical properties of a previously reported luminogen. These results imply, therefore, that this is a general phenomenon that should be taken into account when designing and interpreting the fluorescent outputs of luminescent probes and optoelectronic devices based on fluorescent molecular rotors.

## INTRODUCTION

The development of advanced organic luminogens underpins progress in areas as diverse<sup>1</sup> as fluorescent microscopy,<sup>2</sup> mechanoluminescent materials,<sup>3</sup> and organic light-emitting diodes.<sup>4</sup> In recent years, traditional planar luminogens have been modified<sup>5</sup> to introduce hindered rotation around sterically overcrowded single bonds, juxtaposing 'bright' and 'dark' excited states as a function of rotational and vibrational freedom. The resulting fluorescent molecular rotors have been exploited, among other applications, as materials for photovoltaic devices<sup>6</sup> or as probes to measure viscosities<sup>7</sup> in microheterogeneous environments, such as biological cells.<sup>8</sup>

Some of these molecular rotors exhibit aggregation-induced emission<sup>9</sup> (AIE). That is, they fluoresce weakly, or not at all, when dissolved, but become significantly more emissive in the solid state. In the most extreme cases, photoluminescence quantum yields have been shown<sup>10</sup> to increase from below detection limits in solution to near unity upon aggregation—behavior that is not only desirable for applications in solid state devices, but is also contrary to the aggregation-caused quenching (ACQ) commonly observed for traditional, planar luminogens.<sup>11</sup> A general tactic<sup>9b</sup> used to convert traditional luminogens into fluorescent molecular rotors is to introduce simple aromatic groups, such as phenyl rings<sup>5a, 5c-e</sup>, positioned in close proximity to one another. Steric overcrowding favors non-

planar conformations and introduces hindered single-bond rotations. Tetraarylethylenes,<sup>12</sup> for example, which are archetypal AIE luminogens, can be viewed as stilbenes modified by the addition of two aromatic groups to impart propeller-like arrangements of the rings. Many of the other common AIE motifs<sup>1, 13</sup> are similarly comprised of phenyl rings projecting out from a central core.

The AIE phenomenon, in general, has been attributed<sup>9</sup> to the suppression of non-radiative decay pathways. Confinement in the rigid environment of amorphous aggregates or crystalline solids attenuates vibrations, which leads to enhanced levels of photoluminescence from conformationally restricted excited states. However, an in depth understanding of these excited states and of why AIE luminogens behave differently to ACQ systems is yet to be fully developed.<sup>7e, 9c</sup> To date, the accepted roles of commonly used, monocyclic aromatic rings have generally been limited to creating sterically overcrowded bonds.

Here, we report the unusual fluorescent properties of a series of phenyl-ring molecular rotors, which give us insights into their aggregated states. Not only do the emission intensities of the rotors change under different conditions, but unexpectedly, the *emission energies* are also variable. Two of the rotors emit light from two distinct excited states depending on their environments. We have investigated the luminescent properties of these rotors in solution (i) across a range of temperatures and viscosities, as

well as in the solid state, as part of (ii) thin films, (iii) crystals, and (iv) amorphous aggregates. By analysis of the steady-state and time-resolved emission spectra, solid-state superstructures, and density functional theory (DFT) models, we distinguish (Figure 1) locally excited (LE) state emission from lower energy emission of excited face-to-face aromatic dimers.<sup>14</sup> The flexibility of the rotors and the relative orientations of their peripheral rings influence the likelihood of aromatic dimer formation, which can occur (Figure 1) in an intra- or intermolecular fashion, despite a lack of complementary donor-acceptor interactions. This analysis allows insight into the excited states responsible for emission in aggregates. Moreover, with the aid of DFT calculations, we demonstrate that the formation of face-to-face aromatic dimer states accounts for the behavior of a previously reported multichromic luminogen, suggesting this is a general phenomenon that should be considered when designing and exploiting fluorescent molecular rotors.

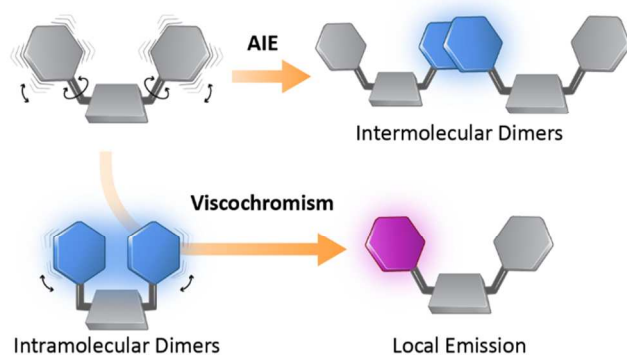


**Figure 1.** Schematic representation of the two processes that lead to face-to-face aromatic dimer formation, observed in the luminescence of the phenyl-ring molecular rotors. In the crystalline or aggregated states, enforced proximity of phenyl rings leads to emission from intermolecular aromatic dimers (shown in blue). A pair of interacting molecules is depicted, representing the local structure in an extended solid-state structure. In solution (i) the excitation may be lost through non-radiative decay, (ii) emission may arise from a relaxed state, brought about by intramolecular pairing (blue) of aromatic rings, or (iii) if dimer formation is prevented, a locally excited state decays by higher energy emission (purple).

## RESULTS AND DISCUSSION

**Chemical Structures of the Molecular Rotors.** *sym*-Triphenylcyclopropene (**Ph<sub>3</sub>C<sub>3</sub>H**), *sym*-pentaphenylcyclopentadiene (**Ph<sub>5</sub>C<sub>5</sub>H**), hexaphenylbenzene (**Ph<sub>6</sub>C<sub>6</sub>**) and *sym*-heptaphenylcycloheptatriene (**Ph<sub>7</sub>C<sub>7</sub>H**) make up (Figure 2) a homologous series of molecular rotors in which a central, unsaturated carbocycle of increasing size is functionalized with a phenyl ring at each vertex. The absence of heteroatoms in these compounds simplifies the analysis of their photophysical properties, while the radial substitution pattern of phenyl rings projecting out from the central carbocycles establish a sterically encumbered environment. Analysis of X-ray crystal structures reveals (Figure 2) that, for the most part, the close proximities of the phenyl rings prevent coplanar conformations. The only exception is **Ph<sub>3</sub>C<sub>3</sub>H**, in which the

central cyclopropene ring lies (Figure 2a) coplanar with two of its relatively unhindered phenyl rings, allowing for favorable orbital overlap and conjugation without unfavorable steric interactions. The propeller-like conformations of phenyl rings that predominate in these compounds would be expected<sup>9b</sup> to impart AIE-type properties. Indeed, **Ph<sub>5</sub>C<sub>5</sub>H**<sup>1b</sup> and **Ph<sub>6</sub>C<sub>6</sub>**<sup>13r</sup> are known to be emissive in the solid state. Although all of the rotors are relatively rigid on account of their cyclic, conjugated cores, **Ph<sub>5</sub>C<sub>5</sub>H** and **Ph<sub>7</sub>C<sub>7</sub>H** possess moderate flexibilities around the single sp<sup>3</sup> center present in their five- or seven-membered ring, respectively. As a result, the cycloheptatriene of **Ph<sub>7</sub>C<sub>7</sub>H** adopts (Figure 2d) a shallow, boat-like conformation in the solid state, in which the phenyl ring bonded to the sp<sup>3</sup> center is oriented above the central carbocycle.

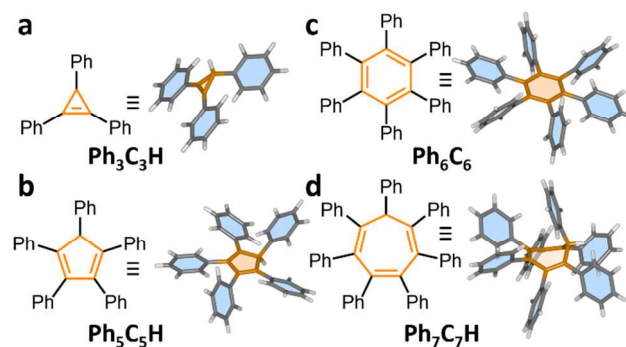


**Figure 2.** Structural formulas and X-ray crystal structures of (a) **Ph<sub>3</sub>C<sub>3</sub>H**, (b) **Ph<sub>5</sub>C<sub>5</sub>H**, (c) **Ph<sub>6</sub>C<sub>6</sub>**, and (d) **Ph<sub>7</sub>C<sub>7</sub>H**, showing the radial orientations of the peripheral phenyl rings around the central carbocycles (orange).

**Two-State Luminescence of Dissolved Rotors.** In order to probe the photoluminescence of the molecular rotors, we acquired steady-state emission spectra<sup>15</sup> of dilute 2-methyltetrahydrofuran (2-MeTHF) solutions. All four of the rotors are only weakly luminescent in solution at room temperature. Upon cooling, however, their emission intensities (Figures S27–S30) increase significantly. Cooling **Ph<sub>7</sub>C<sub>7</sub>H** solutions below 200 K brings about a gradual hypsochromic shift (Figure 3) as the temperature decreases, with concurrent increases in viscosity.<sup>16</sup> The emission maximum ( $E_{em}$ ) shifts from 2.84 eV at 200 K to 3.32 eV at 90 K, undergoing a change in peak shape. These observations lead us to conclude that **Ph<sub>7</sub>C<sub>7</sub>H** emits from two different excited states under these conditions.

**Table 1. Physical Properties of the Molecular Rotors**

Rotor	$E_{\text{ex}}^a$ (eV)	$E_{\text{em}}$ (eV)						QY (%)		$E_{\text{rot}}^b$ (kJ·mol <sup>-1</sup> )	$\tau$ (ns) <sup>c</sup>	
		2-MeTHF	2-MeTHF	Crystal	Film	DMF-H <sub>2</sub> O	MeCN	MeCN-H <sub>2</sub> O	2-MeTHF		2-MeTHF	
		150 K	80 K			(2:8)		(2:8)	290 K		80 K	
<b>Ph<sub>3</sub>C<sub>3</sub>H</b>	3.76	3.40	3.41	3.10	3.17	3.34	– <sup>d</sup>	– <sup>d</sup>	20.61	2.07	2.05	
<b>Ph<sub>5</sub>C<sub>5</sub>H</b>	3.65	2.73	2.91	2.70	2.73	2.76	0.3	14 <sup>e</sup>	30.06	0.61	2.90	
<b>Ph<sub>6</sub>C<sub>6</sub></b>	4.43	3.76	3.83	3.67	3.78	3.83	0.4	4	79.22	0.46	1.63	
<b>Ph<sub>7</sub>C<sub>7</sub>H</b>	3.94	2.90	3.32	3.04	2.77	2.89	0.1	6	42.47	0.91	1.31	

<sup>a</sup>Excitation wavelengths were chosen to match peaks in absorption spectra (Figure S26). <sup>b</sup>Calculated for the most hindered phenyl ring (BMK, Table S2). <sup>c</sup>Values including errors can be found in Tables S7–S9. <sup>d</sup>QYs of **Ph<sub>3</sub>C<sub>3</sub>H** could not be measured accurately on account of ACQ (Figure S46). <sup>e</sup>QY of 3:7 MeCN–H<sub>2</sub>O suspension.

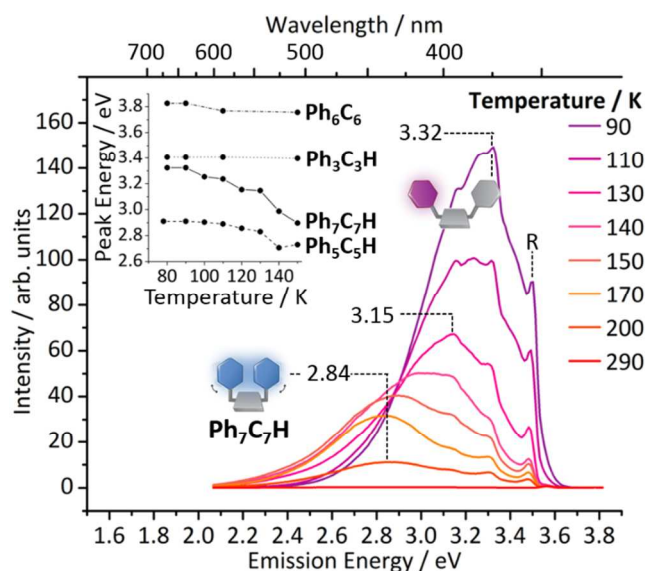


**Figure 3.** Steady-state photoluminescence spectroscopy of **Ph<sub>7</sub>C<sub>7</sub>H** (10  $\mu$ M solution in 2-MeTHF,  $E_{\text{ex}} = 3.94$  eV,  $l = 10$  mm) at a range of temperatures reveals luminescence from two different states. *Inset:* In contrast to **Ph<sub>7</sub>C<sub>7</sub>H**, the emission maxima of **Ph<sub>3</sub>C<sub>3</sub>H** and **Ph<sub>6</sub>C<sub>6</sub>** change very little as temperature is varied, whereas the emission from **Ph<sub>5</sub>C<sub>5</sub>H** undergoes a small hypsochromic shift at low temperature. The peak labeled 'R' is a result of Raman scattering from the solvent.<sup>17</sup>

An excitation energy ( $E_{\text{ex}}$ ) of 3.94 eV is used (Table 1) to excite **Ph<sub>7</sub>C<sub>7</sub>H**. Therefore, the observed peaks correspond to Stokes shifts of 1.04 eV and 0.62 eV, respectively. While the lower energy emission is broad and featureless, there is some vibronic structure apparent for the 3.32 eV peak, indicating<sup>11</sup> that this higher energy emission arises from the LE state, i.e.,  $S_1 \rightarrow S_0$  transitions. No solvatochromism was observed in a series of fluorescence spectra acquired (Figure S31) using solvents of differing polarities, so the shifts in emission do not arise as a result of solvent relaxation. The emission at 2.84 eV must, therefore, correspond to an electronic transition from a relaxed state that resides below the  $S_1$  energy level. A similar, but less pronounced, phenomenon is also observed (Figure 3, inset) for solutions of **Ph<sub>5</sub>C<sub>5</sub>H**, whereby lowering the temperature enhances photoluminescence at  $E_{\text{em}} = 2.73$  eV, which gradual-

ly shifts to  $E_{\text{em}} = 2.91$  eV at 80 K. The emission profiles of **Ph<sub>3</sub>C<sub>3</sub>H** and **Ph<sub>6</sub>C<sub>6</sub>**, on the other hand, do not exhibit changes in peak shapes or significant shifts of the emission maxima in low temperature solutions. Their luminescence is enhanced at lower temperatures, but the observed peaks are consistent with LE state emissions.

We also acquired photoluminescence spectra of 1:5 v/v methylcyclohexane–isopentane (MCH–*i*-pentane) solutions at low temperatures. Unlike the 2-MeTHF solutions ( $T_g = 91$  K), MCH–*i*-pentane solutions ( $T_g = 77$  K) do not freeze under the experimental conditions.<sup>18</sup> No significant differences were observed (Figures S27–30) between the spectra acquired in the two solvents, indicating that the photoluminescence is not influenced by the solvent phase change. Given the low concentrations<sup>20</sup> (1–10  $\mu$ M) of the solutions analyzed by variable temperature and viscosity experiments, we hypothesized that an intramolecular phenomenon was responsible for the emergence of two-state luminescence, prompting us to investigate the available modes of intramolecular motion present in the rotors.

**The Role of Conformational Freedom.** The fluorescence lifetimes,  $\tau$ , of **Ph<sub>7</sub>C<sub>7</sub>H** and **Ph<sub>5</sub>C<sub>5</sub>H** increase (Table 1) at lower temperatures, consistent with the decrease in rates of non-radiative decay reported for other molecular rotors.<sup>21</sup> In order to gain insight into the relative rates of phenyl ring rotations, which presumably contribute to the non-radiative decay, we used DFT methods to calculate (Table S2) the associated energy barriers. Variable temperature NMR spectroscopy measurements revealed (Figure S9) an energy barrier of 39.3 kJ·mol<sup>-1</sup> for the 180° rotation of the most hindered phenyl rings present in **Ph<sub>7</sub>C<sub>7</sub>H**. This measured energy barrier is slightly lower than the calculated energy barrier of 42.5 kJ·mol<sup>-1</sup>, but demonstrates reasonably good agreement between calculation and experiment. The DFT calculations indicate (Table 1) that the phenyl rings of **Ph<sub>6</sub>C<sub>6</sub>** are the most hindered, followed by **Ph<sub>7</sub>C<sub>7</sub>H**, **Ph<sub>5</sub>C<sub>5</sub>H**, and then **Ph<sub>3</sub>C<sub>3</sub>H**. This trend is reflected in temperature-dependent behavior—while the luminescence of **Ph<sub>3</sub>C<sub>3</sub>H** solutions (Figure S27) increases sharply only below about 100 K, for example, **Ph<sub>6</sub>C<sub>6</sub>** solutions begin to emit (Figure S29) brightly from just under 250 K.

The ground state geometries (Figure 4, purple) predicted for the four rotors resemble closely the single crystal X-ray structures (Figure 2). However, there are significant differences in the calculated minimum energy geometries for the  $S_1$  excited states (Figure 4, orange). Calculations were performed using the CAM-B3LYP<sup>22</sup> functional, Def2-SVP basis set, and a C-PCM model to approximate PhMe as solvent. Most noticeably, the minimum energy excited state geometry of **Ph<sub>7</sub>C<sub>7</sub>H** reveals close face-to-face contact between phenyl rings at the 3- and 7-positions of the central cycloheptatriene. This unexpected intramolecular interaction is characterized by a centroid-to-centroid distance of 3.89 Å, aligning the two phenyl rings close together in space and allowing their  $\pi$ -systems to interact.<sup>23</sup> We attribute our observation of two-state luminescence to this interaction—excitation to a LE state can be followed by the formation of a face-to-face aromatic dimer by transannular interaction of the phenyl rings, leading to a relaxed exciton and a red-shifted emission.<sup>24,25</sup> Indeed, more than one distinct minimum was found (Figure S38) for **Ph<sub>7</sub>C<sub>7</sub>H** by sampling the potential energy surface of the first excited state. The temperature- and viscosity-dependent changes in  $E_{em}$  can be rationalized, therefore, by considering that the formation of a relaxed dimer is only possible under conditions that allow for larger amplitude conformational reorganization, i.e., at higher temperatures and lower viscosities. At lower temperatures and higher viscosities, on the other hand, the conformational reorganization is slow on the timescale of the fluorescent emission<sup>16</sup> and higher energy emission from the initial LE state is observed.

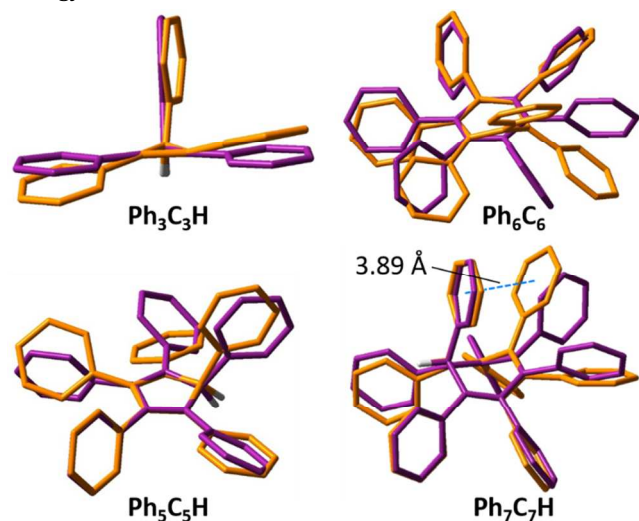


**Figure 4.** DFT minimum energy geometries calculated for the  $S_0$  (purple) and  $S_1$  (orange) electronic states of (a) **Ph<sub>3</sub>C<sub>3</sub>H**, (b) **Ph<sub>5</sub>C<sub>5</sub>H**, (c) **Ph<sub>6</sub>C<sub>6</sub>**, and (d) **Ph<sub>7</sub>C<sub>7</sub>H**, using the CAM-B3LYP<sup>22</sup> functional, Def2-SVP basis set, and a C-PCM model to approximate PhMe as solvent. The dotted blue line illustrates a face-to-face interaction between distal phenyl rings of **Ph<sub>7</sub>C<sub>7</sub>H** in the  $S_1$  state, characterized by a centroid–centroid distance of 3.89 Å and torsion angle of 22°. All H atoms at  $sp^2$ -carbon centers are omitted for clarity.

Rotor **Ph<sub>7</sub>C<sub>7</sub>H**, in particular, is predisposed to undergoing conformational reorganization to form an intramolecular aromatic dimer on account of its  $sp^3$  center, which allows the central cycloheptatriene ring to deviate from planarity.

There are no such transannular interactions evident in the excited state geometries of **Ph<sub>3</sub>C<sub>3</sub>H** or **Ph<sub>6</sub>C<sub>6</sub>**, which is consistent with their more conventional photophysical properties. By drawing analogy to **Ph<sub>7</sub>C<sub>7</sub>H**, the small changes in  $E_{em}$  observed for solutions of **Ph<sub>5</sub>C<sub>5</sub>H** are attributed to weak through-space interactions that develop between the  $\pi$ -systems by conformational reorganization in the excited state, which has (Figure S38) a rather flat potential energy surface. The minimum energy torsional angle between the phenyl rings at the 2- and 3-positions decreases from 72° in the ground state to 55° in the excited state, favoring a weak through-space interaction of the  $\pi$ -electrons.<sup>26</sup>

**Aromatic Interactions in the Solid State.** In order to gain further insight into the excited face-to-face aromatic dimers, we analyzed the photophysical properties of the molecular rotors in the solid state. We measured the fluorescence spectra of crystalline solids, neat films, and 1 wt% dispersions in optically clear poly(methyl methacrylate) (PMMA) and cyclic olefin polymer (ZEONEX<sup>®</sup>) matrices, which were prepared by either drop casting or spin coating polymer–rotor solution mixtures onto quartz substrates. In the rigid environments of the closely packed crystalline solids, the large-amplitude geometric reorganizations required to form the intramolecular face-to-face aromatic dimers are suppressed.<sup>27</sup> Despite this restricted motion, crystalline samples of **Ph<sub>7</sub>C<sub>7</sub>H** emit (Figure 5a) at lower energy compared to the LE state observed in 2-MeTHF at 80 K, indicative of a relaxed excited state. Similarly, crystalline samples of **Ph<sub>5</sub>C<sub>5</sub>H** also fluoresce from partially relaxed excited states – the onset<sup>28</sup> of emission occurs (Figure 5b) about 0.3 eV below that of the LE state observed in 2-MeTHF at 80 K.

Analysis of the solid-state superstructures of **Ph<sub>7</sub>C<sub>7</sub>H** (Figure 5c) and **Ph<sub>5</sub>C<sub>5</sub>H** (Figure 5d) reveals coplanar, face-to-face interactions between the phenyl rings of neighboring molecules in the crystals. Thus, similarly to the relaxation of dilute solutions, the initial excitons evolve to form excited aromatic dimers, but they do so as a result of intermolecular contacts, rather than by intramolecular phenyl-ring dimer formation. Notably, the phenyl rings involved in these interactions in the solid state are different from those in solution – e.g., the phenyl group at the  $sp^3$ -carbon center of **Ph<sub>7</sub>C<sub>7</sub>H**, which takes part in the face-to-face aromatic dimer in solution, is only in close contact with the edges of neighboring aromatic rings in the crystal (Figure S22). Nevertheless, the spectroscopic data show that the photophysical outcome is similar. The exciton relaxes from the  $S_1$  energy level by sharing the excitation energy across two phenyl rings, reaching an excited state that resides at a similar energy to that observed in solution. Neither **Ph<sub>3</sub>C<sub>3</sub>H** nor **Ph<sub>6</sub>C<sub>6</sub>** display any evidence of relaxed emission in the solid state, which is consistent with the lack (Figures S12 and S18) of significant face-to-face contacts of their conjugated phenyl rings.

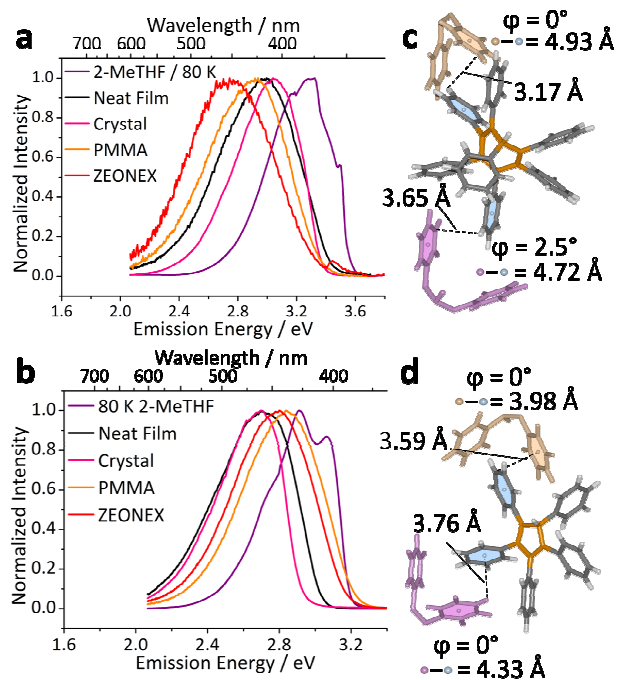


**Figure 5.** Emission profiles of (a)  $\text{Ph}_7\text{C}_7\text{H}$  and (b)  $\text{Ph}_5\text{C}_5\text{H}$  in crystalline and amorphous condensed phases are contrasted with the emission from frozen 2-MeTHF solutions. Solid-state packing interactions are shown for the carbocycles in (c) and (d), respectively. Colored spheres denote centroids and  $\phi$  denotes the torsion angles between the planes defined by the atoms of the benzene rings.

The neat films also emit from aromatic dimer states. Emission onsets of both  $\text{Ph}_7\text{C}_7\text{H}$  and  $\text{Ph}_5\text{C}_5\text{H}$  films are close (Figure 5) to those observed for crystalline samples, although the peaks are broader on account of the greater inhomogeneity in the amorphous samples. Slightly higher energy emissions are observed from the films, which are presumably a result of the less efficient packing in the amorphous films reducing the likelihood of close face-to-face contacts between phenyl rings.

By preparing polymer blends of the rotors, we dilute their concentrations in the films, which would be expected to diminish the presence of intermolecular dimers and favor fluorescence from LE states. The emission onsets of the 1 wt%  $\text{Ph}_5\text{C}_5\text{H}$  films do indeed coincide with the LE state emission observed from the frozen 2-MeTHF solution, showing that the rotor is well-dispersed in the PMMA or ZEONEX<sup>®</sup> and is, therefore, prevented from forming intermolecular aromatic interactions. Atomic force microscopy (AFM) images (Figure 6) reveal that both of the spin-coated  $\text{Ph}_5\text{C}_5\text{H}$ -polymer films have smooth topographies, supporting the notion that the films are homogeneous and the  $\text{Ph}_5\text{C}_5\text{H}$  is evenly distributed.

In contrast to  $\text{Ph}_5\text{C}_5\text{H}$ , the fluorescence of the 1 wt% films of  $\text{Ph}_7\text{C}_7\text{H}$  appear to be dominated (Figure 5a) by relaxed dimer emission. The emission maxima move (Figure S25) in response to changes in temperature, similarly to the behavior observed (Figure 3) for 2-MeTHF solutions,

which is indicative of similar intramolecular phenyl-ring dimers. Notably, however, the higher viscosity environment of the polymer matrices causes these changes to occur at higher temperatures. AFM topographical images of the  $\text{Ph}_7\text{C}_7\text{H}$ -ZEONEX<sup>®</sup> film show (Figure 6d) a surface that is significantly rougher than the other films. There are visible protrusions of  $\sim 20$  nm, suggesting that the  $\text{Ph}_7\text{C}_7\text{H}$  is not well dispersed, but has formed some small aggregates.<sup>29</sup> The values for surface roughness,  $R_q$ , were measured to be 153.6 pm for the PMMA film and 212.5 pm for ZEONEX<sup>®</sup>. Moreover, the emission from the  $\text{Ph}_7\text{C}_7\text{H}$ -ZEONEX<sup>®</sup> film is slightly red-shifted (Figure 5a) relative to the PMMA film. In addition to the intramolecular interactions, therefore, there is also some contribution from intermolecular interactions present in the  $\text{Ph}_7\text{C}_7\text{H}$ -ZEONEX<sup>®</sup> film.

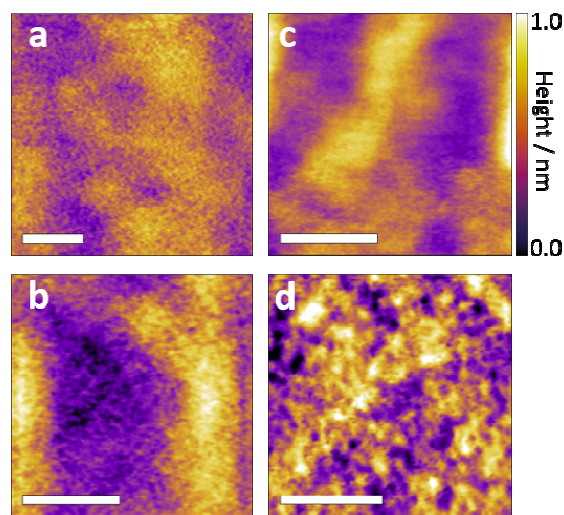


**Figure 6.** AFM images of spin-coated films of (a)  $\text{Ph}_5\text{C}_5\text{H}$  in PMMA, (b)  $\text{Ph}_5\text{C}_5\text{H}$  in ZEONEX<sup>®</sup>, (c)  $\text{Ph}_7\text{C}_7\text{H}$  in PMMA, and (d)  $\text{Ph}_7\text{C}_7\text{H}$  in ZEONEX<sup>®</sup>. Scale bars = 200 nm.

**Effects of Aggregation.** Distinguishing the interactions between molecules during the aggregation process is crucial to developing a robust understanding of AIE processes.<sup>30</sup> Having established the luminescence pathways for the phenyl-ring molecular rotors in solution and bulk solid phases, we investigated the emissive properties (Figures 7 and S34–S37) of nanoaggregates prepared by adding a poor solvent (water) to dimethylformamide (DMF) and MeCN solutions of the rotors.

Based on emission intensities alone, it is clear that  $\text{Ph}_3\text{C}_3\text{H}$  undergoes ACQ, whereas the other three rotors are AIE active. Apart from  $\text{Ph}_3\text{C}_3\text{H}$ , the photoluminescence quantum yields (QYs) of the rotors increase upon precipitation from MeCN (Table 1) or DMF (Table S10) solutions. The differing behaviors of the rotors are dictated by the preferred orientations of their phenyl rings and the geometrical restraints placed on their interactions. The least hindered rotor,  $\text{Ph}_3\text{C}_3\text{H}$ , preferentially takes up (Figure 2a) a coplanar, stilbene-like conformation, which leads to static quenching<sup>11</sup> of fluorescence upon aggregation. Aggregates of  $\text{Ph}_6\text{C}_6$ , on the other hand, display conventional AIE characteristics, emitting with increasing brightness as the concentration of water is increased, but without undergoing

variation in  $E_{em}$ . Recalling that **Ph<sub>6</sub>C<sub>6</sub>** is the most hindered (Table 1) of the four luminogens (i) the peripheral phenyl groups are held out of the plane of the central benzene, but (ii) they are also unable to undergo either intra- or intermolecular pairing in the nanoaggregates.

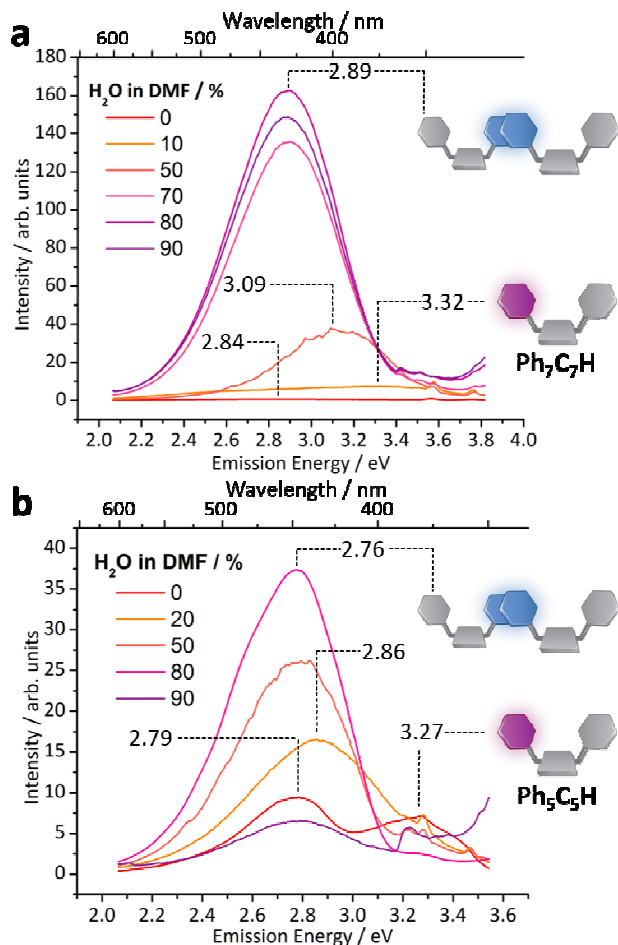


**Figure 7.** Steady-state photoluminescence spectra of (a) **Ph<sub>7</sub>C<sub>7</sub>H** and (b) **Ph<sub>5</sub>C<sub>5</sub>H** suspensions in H<sub>2</sub>O-DMF ( $E_{ex} = 3.94$  eV [**Ph<sub>7</sub>C<sub>7</sub>H**] /  $3.65$  eV [**Ph<sub>5</sub>C<sub>5</sub>H**],  $l = 10$  mm,  $T = 298$  K). As increasing proportions of H<sub>2</sub>O are added to the DMF solutions, emissive aggregates are formed. At high water contents, the emission energies are similar to the relaxed phenyl-dimer states observed in crystalline samples, which we ascribe to intermolecular interactions in the aggregates. Low intensity, higher energy emissions are observed from suspensions with lower water content (e.g., 10–50% for **Ph<sub>7</sub>C<sub>7</sub>H**), consistent with some localized emission. Small, sharp peaks above 3.20 eV in Figure 7b correspond to Raman scattering from the solvent.

Unlike **Ph<sub>3</sub>C<sub>3</sub>H** and **Ph<sub>6</sub>C<sub>6</sub>**, the AIE spectroscopic characteristics of **Ph<sub>7</sub>C<sub>7</sub>H** (Figure 7a) and **Ph<sub>5</sub>C<sub>5</sub>H** (Figure 7b) are dominated by excited face-to-face aromatic dimers. Dynamic light scattering (DLS) measurements show an increase in scattering (Figure S23), consistent with the formation of nanoaggregates under these conditions. Intermolecular interactions, similar to those observed (Figure 6) in the crystals, are responsible for the relaxed emission.

Comparison of the UV-vis spectra of solutions and aggregated mixtures shows (Figure S26) red shifts in the absorption peaks, arising from the intermolecular aromatic interactions. In DMF solution, **Ph<sub>5</sub>C<sub>5</sub>H** displays two distinct fluorescence peaks—one at  $E_{em} = 3.27$  eV that is assigned to the LE state, and the other at  $E_{em} = 2.76$  eV that is characteristic of relaxed phenyl-ring dimers. Similarly, there is some contribution from the LE state to emissions from **Ph<sub>7</sub>C<sub>7</sub>H** suspensions at low water contents, e.g., 10% water in DMF, as evidenced by a low intensity peak at  $E_{em} = 3.32$  eV. However, the strongly emissive aggregates that form at higher water contents (i.e., above 50%) display  $E_{em}$  values and onset energies that match the relaxed excited states discussed above.

**Discussion.** Shifts in the emission wavelengths of fluorophores under different experimental conditions are not uncommon. Depending on the structure of the fluorophore, they may be attributed to phenomena such as (i) solvent relaxation, (ii) internal charge transfer, or (iii) changes in the Coulombic coupling of aggregates (i.e., J- or H-aggregation).<sup>11,22</sup> But these effects are normally only prominent for fluorophores that (i) are polar, (ii) contain donor and acceptor groups, or (iii) are comprised of a large, planar  $\pi$ -surface. The molecular rotors described here are nonplanar, apolar hydrocarbons—they lack any of the features that would normally be associated with variable  $E_{em}$  in different environments, so the significant shifts between the LE and relaxed emissions of **Ph<sub>7</sub>C<sub>7</sub>H** and **Ph<sub>5</sub>C<sub>5</sub>H** are surprising.<sup>24</sup> Observation of the aromatic dimer excited states for these rotors, therefore, raises the questions “is this a general phenomenon?” and “which factors favor formation of the aromatic dimers?”.

In answer to the first question, a survey of previously reported data for phenyl-ring luminogens shows that, in some cases<sup>9c, 13g, 13k, 13n, 13p</sup>, there are spectroscopic shifts upon formation of nanoaggregates that are comparable to our observations (Figure 7). So, it appears that the excited-state aromatic dimer formation may be a general phenomenon that is not limited to the carbocyclic rotors reported here. For example, 2,2'-biindene **1** (Figure 8), which was described by Tian et al. in 2011, shows distinct peaks at  $E_{em} = 2.58$  eV and  $E_{em} = 3.00$  eV in its photoluminescence spectra in the solution and aggregated states, respectively.<sup>13g</sup> Rotation around the central single bond of **1** interconverts (Figure 8a) the *anti*- and *syn*-isomers. Our calculations indicate (Figure 8b) that *anti*-**1** is preferred in the ground state, but a *syn*-conformation becomes favorable in the excited state, which is accompanied by a face-to-face interaction between the phenyl rings. Therefore, the hypsochromic shift<sup>13g</sup> brought about by aggregation can be attributed to intramolecular aromatic dimer formation in solution. The dimer formation is prevented by the restricted environment of the aggregates, leading to higher energy emission from the LE state.

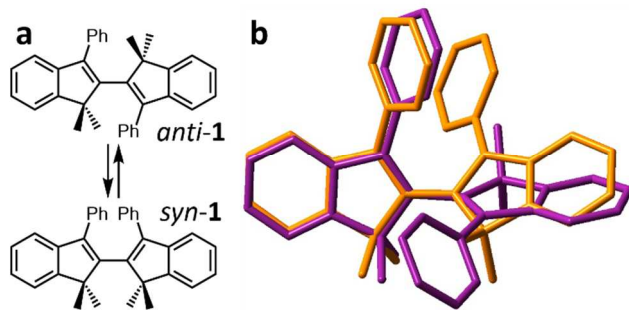


**Figure 8.** (a) Previously reported 2,2'-biindene **1** undergoes hypsochromic shift in its fluorescence upon aggregation. (b) Our DFT modelling of the S<sub>0</sub> (purple) and S<sub>1</sub> (orange) electronic states suggests this effect results from a through-space aromatic dimer in solution, which cannot form in the aggregated-state. All H atoms are omitted for clarity.

On the other hand, there are, of course, many examples of molecular rotors that do not form aromatic dimer excited states. There does not seem to be any reported data that suggests the widely used tetraarylethylenes<sup>12</sup> are subject to this phenomenon, for example, and nor are **Ph<sub>3</sub>C<sub>3</sub>H** and **Ph<sub>6</sub>C<sub>6</sub>**, according to the data described here.

At this stage, it is difficult to delineate the structural characteristics that favor aromatic dimers over LE in the excited states. In the solid state, weak noncovalent interactions dictate the packing and ultimately determine whether or not the aromatic groups of neighboring molecules are held together, promoting intermolecular aromatic dimer states. However, analysis of the series of rotors reported here does hint that the degree of conformational flexibility is an important factor for intramolecular dimer formation<sup>31</sup> – there must be sufficient flexibility to allow the faces of the aromatic rings to come into contact, while also maintaining a sterically crowded environment to minimize non-radiative decay. Moreover, an intramolecular aromatic dimer may form in the excited state, even when the relevant conformation is not favored in the ground state. It is well-established that weak ground-state interactions<sup>32</sup> between phenyl rings stabilize<sup>33</sup> the secondary structures of proteins, and that the interaction potential energy surface of two aromatic rings is relatively flat. So, the stabilizing effect of a shared exciton could provide the driving force to alter minimum energy conformations in this way.

Overall, our results indicate that simple aromatic rings present in molecular rotors can do more than merely introduce steric hindrance. Their interactions can lead to emission from previously unexpected excited-state dimers. This phenomenon should be considered, therefore, when designing and interpreting the behavior of fluorescent molecular rotors—even those based on unfunctionalized hydrocarbon backbones. Shifts in emission energy need not always be attributed simply to 'solvent effects'. At a time when molecular rotors are being used more frequently as probes for quantitative measurements, it is important to have a full understanding of how their photophysical output can respond to changes in their environments.

## CONCLUSION

In summary, by investigating the properties of a series of phenyl-ring molecular rotors, we have identified photoluminescence from through-space aromatic dimers. The dimers form in either an intra- or intermolecular fashion between small, unfunctionalized aromatic rings, leading to relaxed excited states. Previously, fluorophores lacking large, flat  $\pi$ -systems or polarized functional groups have generally not been expected to undergo such significant relaxation.<sup>24</sup> The least hindered rotor, **Ph<sub>3</sub>C<sub>3</sub>H**, shows the characteristics of a traditional fluorophore, undergoing quenching in the solid state, while the most hindered, **Ph<sub>6</sub>C<sub>6</sub>**, undergoes AIE. Both fluoresce from the LE state under all conditions. Rotors **Ph<sub>7</sub>C<sub>7</sub>H** and **Ph<sub>5</sub>C<sub>5</sub>H**, on the other hand, emit from the LE state at very low temperatures or high viscosities, but otherwise luminesce from through-space aromatic dimer states. Intramolecular dimer formation appears to be influenced by the degree of conformational flexibility present in the rotors in solution, while the intermolecular excited states are governed by the interdigitation of the rotors in the solid state. Our results illustrate that, given the right spatial orientations, interactions between simple aromatic rings are sufficient to cause significant shifts in photoluminescence energies. DFT modeling and analysis of previously published spectroscopic data suggest that this is a general phenomenon. Care should be taken, therefore, when designing and interpreting the results of sensing systems or optoelectronic devices based around similar molecular rotors.

## ASSOCIATED CONTENT

### Supporting Information

The Supporting Information is available free of charge on the ACS Publications Website at DOI: XX.XXXX/XXXX.XXXXXXX.

Synthetic procedures, characterization data, X-ray crystallographic data, experimental methods, additional optical data, theoretical calculations, and time-resolved fluorescence (PDF)

## AUTHOR INFORMATION

### Corresponding Authors

alyssa.j.avestro@durham.ac.uk  
a.p.monkman@durham.ac.uk  
paul.mcgonigal@durham.ac.uk

### Present Addresses

<sup>†</sup>Department of Inorganic Chemistry, University of Chemistry and Technology Prague, Technická 5, 16628 Prague 6, Czech Republic.

### Notes

The authors declare no competing financial interests.

## ACKNOWLEDGMENT

J.S. gratefully acknowledges the support of an Experientia Foundation Fellowship and an EPSRC Impact Acceleration Account, as well as access to Computational resources provided by the CESNET LM2015042 and the CERIT Scientific Cloud LM2015085, provided under the programme "Projects of Large Research, Development, and Innovations Infrastructures". M.K.E. and H.F.H. acknowledge the EU's Horizon 2020 for funding the PHEBE project under grant no. 641725. A.-J.A. thanks the Royal Commission for the Exhibition of 1851 for

the award of a Science and Engineering Research Fellowship. A.P.M. acknowledges the EPSRC for funding under grant number EP/L02621X/1. P.R.M. acknowledges the support of an EPSRC First Grant (EP/N029992/1) and a Royal Society Research Grant (RG150558). The authors thank Dr Lars-Olof Pålsson, Dr Qing He, Prof David Parker, and Prof Andy Beeby for access to instruments and useful discussions.

## REFERENCES

- (a) Zhao, Y. S.; Fu, H.; Hu, F.; Peng, A. D.; Yao, J. *Adv. Mater.* **2007**, *19*, 3554; (b) Xiao, Y.; Peng, H. D.; Wang, J. Y.; Wu, H. D.; Liu, Z. H.; Pan, G. B. *Phys. Chem. Chem. Phys.* **2016**, *18*, 7019.
- (a) Shin, W. S.; Lee, M.-G.; Verwilst, P.; Lee, J. H.; Chi, S.-G.; Kim, J. S. *Chem. Sci.* **2016**, *7*, 6050; (b) Nicol, A.; Qin, W.; Kwok, R. T. K.; Burkhartsmeyer, J. M.; Zhu, Z.; Su, H.; Luo, W.; Lam, J. W. Y.; Qian, J.; Wong, K. S.; Tang, B. Z. *Chem. Sci.* **2017**, *8*, 4634; (c) Cheng, Y.; Sun, C.; Ou, X.; Liu, B.; Lou, X.; Xia, F. *Chem. Sci.* **2017**, *8*, 4571.
- (a) Yu, T.; Ou, D.; Yang, Z.; Huang, Q.; Mao, Z.; Chen, J.; Zhang, Y.; Liu, S.; Xu, J.; Bryce, M. R.; Chi, Z. *Chem. Sci.* **2017**, *8*, 1163; (b) Okazaki, M.; Takeda, Y.; Data, P.; Pander, P.; Higginbotham, H.; Monkman, A. P.; Minakata, S. *Chem. Sci.* **2017**, *8*, 2677; (c) Qi, Q. K.; Liu, Y. F.; Fang, X. F.; Zhang, Y. M.; Chen, P.; Wang, Y.; Yang, B.; Xu, B.; Tian, W. J.; Zhang, S. X. A. *RSC Adv.* **2013**, *3*, 7996; (d) Luo, X. L.; Zhao, W. J.; Shi, J. Q.; Li, C. H.; Liu, Z. P.; Bo, Z. S.; Dong, Y. Q.; Tang, B. Z. *J. Phys. Chem. C* **2012**, *116*, 21967.
- (a) Zhao, Z.; Chen, S.; Lam, J. W. Y.; Wang, Z.; Lu, P.; Mahtab, F.; Sung, H. H. Y.; Williams, I. D.; Ma, Y.; Kwok, H. S.; Tang, B. Z. *J. Mater. Chem.* **2011**, *21*, 7210; (b) Tsujimoto, H.; Ha, D. G.; Markopoulos, G.; Chae, H. S.; Baldo, M. A.; Swager, T. M. *J. Am. Chem. Soc.* **2017**, *139*, 4894; (c) Tang, C. W.; Vanslyke, S. A. *Appl. Phys. Lett.* **1987**, *51*, 913.
- (a) Xie, Z.; Yang, B.; Li, F.; Cheng, G.; Liu, L.; Yang, G.; Xu, H.; Ye, L.; Hanif, M.; Liu, S.; Ma, D.; Ma, Y. *J. Am. Chem. Soc.* **2005**, *127*, 14152; (b) Lee, K. H.; Kwon, Y. S.; Lee, J. Y.; Kang, S.; Yook, K. S.; Jeon, S. O.; Lee, J. Y.; Yoon, S. S. *Chem.—Eur. J.* **2011**, *17*, 12994; (c) Mazumdar, P.; Das, D.; Sahoo, G. P.; Salgado-Moran, G.; Misra, A. *Phys. Chem. Chem. Phys.* **2014**, *16*, 6283; (d) Sharma, K.; Kaur, S.; Bhalla, V.; Kumar, M.; Gupta, A. *J. Mater. Chem. A* **2014**, *2*, 8369; (e) Li, J.; Li, P.; Wu, J.; Gao, J.; Xiong, W. W.; Zhang, G.; Zhao, Y.; Zhang, Q. *J. Org. Chem.* **2014**, *79*, 4438.
- Wang, C.; Liu, Z.; Li, M.; Xie, Y.; Li, B.; Wang, S.; Xue, S.; Peng, Q.; Chen, B.; Zhao, Z.; Li, Q.; Ge, Z.; Li, Z. *Chem. Sci.* **2017**, *8*, 3750.
- (a) Kuimova, M. K.; Botchway, S. W.; Parker, A. W.; Balaz, M.; Collins, H. A.; Anderson, H. L.; Suhling, K.; Ogilby, P. R. *Nature Chem.* **2009**, *1*, 69; (b) Liu, T.; Liu, X.; Spring, D. R.; Qian, X.; Cui, J.; Xu, Z. *Sci. Rep.* **2014**, *4*, 5418; (c) Vyšniauskas, A.; Qurashi, M.; Gallop, N.; Balaz, M.; Anderson, H. L.; Kuimova, M. K. *Chem. Sci.* **2015**, *6*, 5773; (d) Sherin, P. S.; López-Duarte, I.; Dent, M. R.; Kubánková, M.; Vyšniauskas, A.; Bull, J. A.; Reshetnikova, E. S.; Klymchenko, A. S.; Tsentelovich, Y. P.; Kuimova, M. K. *Chem. Sci.* **2017**, *8*, 3523; (e) Qian, H.; Cousins, M. E.; Horak, E. H.; Wakefield, A.; Liptak, M. D.; Aprahamian, I. *Nature Chem.* **2017**, *9*, 83; (f) Vyšniauskas, A.; Ding, D.; Qurashi, M.; Boczarow, I.; Balaz, M.; Anderson, H. L.; Kuimova, M. K. *Chem.—Eur. J.* **2017**, *23*, 11001.
- Qian, J.; Tang, B. Z. *Chem* **2017**, *3*, 56.
- (a) Mei, J.; Hong, Y.; Lam, J. W.; Qin, A.; Tang, Y.; Tang, B. Z. *Adv. Mater.* **2014**, *26*, 5429; (b) Mei, J.; Leung, N. L.; Kwok, R. T.; Lam, J. W.; Tang, B. Z. *Chem. Rev.* **2015**, *115*, 11718; (c) Xiong, J. B.; Feng, H. T.; Sun, J. P.; Xie, W. Z.; Yang, D.; Liu, M.; Zheng, Y. S. *J. Am. Chem. Soc.* **2016**, *138*, 11469.
- Ng, J. C. Y.; Liu, J.; Su, H.; Hong, Y.; Li, H.; Lam, J. W. Y.; Wong, K. S.; Tang, B. Z. *J. Mater. Chem. C* **2014**, *2*, 78.
- Lakowicz, J. R. *Principles of Fluorescence Spectroscopy*. 3rd ed.; Springer: New York, 2006.
- (a) Dong, Y.; Lam, J. W. Y.; Qin, A.; Liu, J.; Li, Z.; Tang, B. Z.; Sun, J.; Kwok, H. S. *Appl. Phys. Lett.* **2007**, *91*, 011111; (b) Zhao, Z.; Lam, J. W. Y.; Tang, B. Z. *Curr. Org. Chem.* **2010**, *14*, 2109; (c) Zhao, Z.; Lam, J. W. Y.; Tang, B. Z. *J. Mater. Chem.* **2012**, *22*, 23726; (d) Qi, Q.; Qian, J.; Ma, S.; Xu, B.; Zhang, S. X.; Tian, W. *Chem.—Eur. J.* **2015**, *21*, 1149; (e) Li, Y.; Liu, Y.; Zhou, H.; Chen, W.; Mei, J.; Su, J. *Chem.—Eur. J.* **2017**, *23*, 9280.
- (a) Kido, J.; Shionoya, H.; Nagai, K. *Appl. Phys. Lett.* **1995**, *67*, 2281; (b) Luo, J.; Xie, Z.; Lam, J. W. Y.; Cheng, L.; Chen, H.; Qiu, C.; Kwok, H. S.; Zhan, X.; Liu, Y.; Zhuc, D.; Tang, B. Z. *Chem. Commun.* **2001**, 1740; (c) Gao, X.-C.; Cao, H.; Huang, L.; Huang, Y.-Y.; Zhang, B.-W.; Huang, C.-H. *Appl. Surf. Sci.* **2003**, *210*, 183; (d) Chen, J.; Xu, B.; Ouyang, X.; Tang, B. Z.; Cao, Y. *J. Phys. Chem. A* **2004**, *108*, 7522; (e) Zhao, Y. S.; Peng, A.; Fu, H.; Ma, Y.; Yao, J. *Adv. Mater.* **2008**, *20*, 1661; (f) Shimizu, M.; Tatsumi, H.; Mochida, K.; Shimono, K.; Hiyama, T. *Chem.—Asian J.* **2009**, *4*, 1289; (g) Zhang, Z. Y.; Xu, B.; Su, J. H.; Shen, L. P.; Xie, Y. S.; Tian, H. *Angew. Chem. Int. Ed.* **2011**, *50*, 11654; (h) Feng, J.; Chen, X.; Han, Q.; Wang, H.; Lu, P.; Wang, Y. *J. Lumin.* **2011**, *131*, 2775; (i) Yang, L.; Ye, J.; Xu, L.; Yang, X.; Gong, W.; Lin, Y.; Ning, G. *RSC Adv.* **2012**, *2*, 11529; (j) Zhang, X.; Ye, J.; Xu, L.; Yang, L.; Deng, D.; Ning, G. *J. Lumin.* **2013**, *139*, 28; (k) Zhao, Z.; He, B.; Nie, H.; Chen, B.; Lu, P.; Qin, A.; Tang, B. Z. *Chem. Commun.* **2014**, *50*, 1131; (l) Kojima, T.; Hiraoka, S. *Org. Lett.* **2014**, *16*, 1024; (m) Wunderlich, K.; Larsen, A.; Marakis, J.; Fytas, G.; Klapper, M.; Müllen, K. *Small* **2014**, *10*, 1914; (n) Zhang, J.; Xu, B.; Chen, J.; Ma, S.; Dong, Y.; Wang, L.; Li, B.; Ye, L.; Tian, W. *Adv. Mater.* **2014**, *26*, 739; (o) Chang, Z. F.; Jing, L. M.; Wei, C.; Dong, Y. P.; Ye, Y. C.; Zhao, Y. S.; Wang, J. L. *Chem.—Eur. J.* **2015**, *21*, 8504; (p) Zhu, Q.; Zhang, Y.; Nie, H.; Zhao, Z.; Liu, S.; Wong, K. S.; Tang, B. Z. *Chem. Sci.* **2015**, *6*, 4690; (q) Lungerich, D.; Reger, D.; Hçlzel, H.; Riedel, R.; Martin, M. M. J. C.; Hampel, F.; Jux, N. *Angew. Chem. Int. Ed.* **2016**, *55*, 5602; (r) Vij, V.; Bhalla, V.; Kumar, M. *Chem. Rev.* **2016**, *116*, 9565; (s) Zhang, Y.; He, B.; Luo, W.; Peng, H.; Chen, S.; Hu, R.; Qin, A.; Zhao, Z.; Tang, B. Z. *J. Mater. Chem. C* **2016**, *4*, 9316; (t) Yang, J.; Ren, Z.; Xie, Z.; Liu, Y.; Wang, C.; Xie, Y.; Peng, Q.; Xu, B.; Tian, W.; Zhang, F.; Chi, Z.; Li, Q.; Li, Z. *Angew. Chem. Int. Ed.* **2017**, *56*, 880.
- We use the term 'dimer' to describe the pairs of similar (but not chemically equivalent) phenyl rings that exhibit close, face-to-face aromatic interactions through either an intra- or intermolecular contacts. To avoid confusion, we have chosen not to use terms such as 'excimer', which normally describes an intermolecular dimer formed in the excited state, and other more specific terminology.
- Emission spectra are reported in eV and are Jacobian corrected to allow meaningful comparisons of Stokes shifts between compounds, see: Mooney, J.; Kambhampati, P. *J. Phys. Chem. Lett.* **2013**, *4*, 3316.
- Previous reports have shown that the increasing viscosities of cold 2-MeTHF solutions can lead to restriction of molecular rotation, see: Lewis, F. D.; Liu, W. Z. *J. Phys. Chem. A* **2002**, *106*, 1976.
- Durig, J. R.; Kizer, K. L.; Karriker, J. M. *J. Raman Spectrosc.* **1973**, *1*, 17.
- Glass transition temperatures ( $T_g$ ) have been determined previously for 2-MeTHF and 1:5 v/v MCH-*i*-pentane, see: (a) Kligler, D. S. *Ultrasensitive Laser Spectroscopy*. 1st ed.; Academic Press: New York, 1983; (b) Mizukami, M.; Fujimori, H.; Oguni, M. *Prog. Theor. Phys. Suppl.* **1997**, *79*.
- (a) Mendelovici, E.; Frost, R. L.; Klopogge, T. *J. Raman Spectrosc.* **2000**, *31*, 1121; (b) Matsuura, H.; Miyazawa, T.; Hiraishi, M. *Spectrochim. Acta Part A Mol. Spectrosc.* **1972**, *A28*, 2299.
- The average expected intermolecular distances at these concentrations is approximately 100 nm. Variable concentration studies show a lack of concentration-dependent shifts in emission that would be expected for an intermolecular phenomenon. See Figure S32.
- Kuimova, M. K.; Yahioglu, G.; Levitt, J. A.; Suhling, K. *J. Am. Chem. Soc.* **2008**, *130*, 6672.
- Wiggins, P.; Williams, J. A.; Tozer, D. J. *J. Chem. Phys.* **2009**, *131*, 091101.
- It is well known that the wavelengths of light emitted from traditional, planar organic chromophores are dependent on the overlap and orientation of  $\pi$ -surfaces. Although this analysis is usually applied to large, polycyclic  $\pi$ -systems, such as perylene, it

1 may also be applied to simple phenyl rings, see: Hestand, N. J.;  
2 Spano, F. C., *Acc. Chem. Res.* **2017**, *50*, 341.

3 24. For precedent supporting the assignment of excimer-like  
4 states in phenyl-ring pairs, see: (a) Hirayama, F. *J. Chem. Phys.*  
5 **1965**, *42*, 3163; (b) Nishihara, T.; Kaneko, M. *Makromol. Chem.*  
6 **1969**, *124*, 84; (c) Avouris, P.; Ashraf El-Bayoumi, M. *Chem. Phys.*  
7 *Lett.* **1973**, *20*, 59; (d) Tsai, F. J.; Torkelson, J. M. *Polymer* **1988**, *29*,  
8 1004.

9 25. While this article was under review, a manuscript was submitted  
10 detailing the interactions between aromatic rings in  
11 tetraarylethanes: Zhang, H.; Zheng, X.; Xie, N.; He, Z.; Liu, J.; Leung,  
12 N. L. C.; Niu, Y.; Huang, X.; Wong, K. S.; Kwok, R. T. K.; Sung H. H. Y.;  
13 Williams, I. D.; Qin, A.; Lam, J. W. Y.; Tang, B. Z. *J. Am. Chem. Soc.*  
14 **2017**, *139*, 16264.

15 26. Through-space electronic interactions have been observed for  
16 macrocycles that constrain aromatic systems at torsional angles  
17 of  $\sim 60^\circ$ , see: Schneebeli, S. T.; Frascioni, M.; Liu, Z.; Wu, Y.; Gard-  
18 ner, D. M.; Strutt, N. L.; Cheng, C.; Carmieli, R.; Wasielewski, M. R.;  
19 Stoddart, J. F. *Angew. Chem. Int. Ed.* **2013**, *52*, 13100.

20 27. Rapid, large-amplitude motions are uncommon in crystals, but  
21 they can be engineered by designing crystalline solids with large  
22 cavities, see: (a) Jiang, X.; O'Brien, Z. J.; Yang, S.; Lai, L. H.;  
23 Buenaflor, J.; Tan, C.; Khan, S.; Houk, K. N.; Garcia-Garibay, M. A. *J.*  
24 *Am. Chem. Soc.* **2016**, *138*, 4650; (b) Catalano, L.; Perez-Estrada,  
25 S.; Wang, H. H.; Ayitou, A. J. L.; Khan, S. I.; Terraneo, G.; Metran-  
26 golo, P.; Brown, S.; Garcia-Garibay, M. A. *J. Am. Chem. Soc.* **2017**,  
27 *139*, 843.

28. Onset values are used as they better represent the highest  
29 energy transition of species that have a broadband emission, e.g.,  
30 charge-transfer states, see: (a) Etherington, M. K.; Gibson, J.; Hig-  
31 ginbotham, H. F.; Penfold, T. J.; Monkman, A. P. *Nature Commun.*  
32 **2016**, *7*, 13680; (b) Turro, N. J.; Ramamurthy, V.; Scaiano, J. C.  
33 *Principles of Molecular Photochemistry: An Introduction*. 1st ed.;  
University Science Books: USA, 2009.

29. See Section 16 of the Supporting Information.

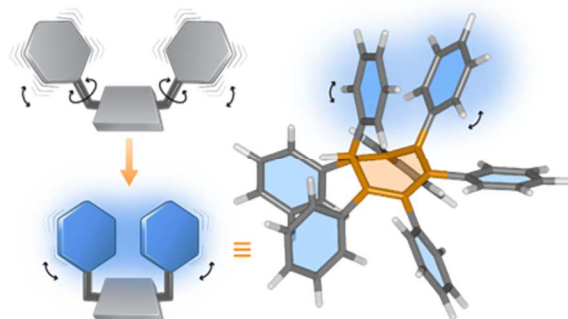
30. Through space interactions of  $\pi$ -systems have previously been  
31 shown to influence the emission of AIE-active luminogens, based  
32 upon the conventional interactions of donor-acceptor pairs or  
33 large polycyclic systems: (a) Dai, Q.; Liu, W.; Zeng, L.; Lee, C.-S.;  
Wu, J.; Wang, P. *CrystEngComm* **2011**, *13*, 4617; (b) Liu, Y.; Zhang,  
Y.; Wu, X.; Lan, Q.; Chen, C.; Liu, S.; Chi, Z.; Jiang, L.; Chen, X.; Xu, J. *J.*  
*Mater. Chem. C* **2014**, *2*, 1068. See also ref 4a.

31. The size of polystyrene macrocycles has been found to dictate  
32 the relative amount of excimer-like fluorescence. This effect has  
33 been ascribed to changes in the relative orientations of phenyl  
rings, see: Gan, Y. D.; Dong, D. H.; Carlotti, S.; Hogen-Esch, T. E. *J.*  
*Am. Chem. Soc.* **2000**, *122*, 2130.

32. Martinez, C. R.; Iverson, B. L. *Chem. Sci.* **2012**, *3*, 2191.

33. (a) Burley, S. K.; Petsko, G. A. *Science* **1985**, *229*, 23; (b) Sun, S.;  
Bernstein, E. R. *J. Phys. Chem.* **1996**, *100*, 13348; (c) Aravinda, S.;  
Shamala, N.; Das, C.; Sriranjini, A.; Karle, I. L.; Balaram, P. *J. Am.*  
*Chem. Soc.* **2003**, *125*, 5308.

## Table of Contents Graphic



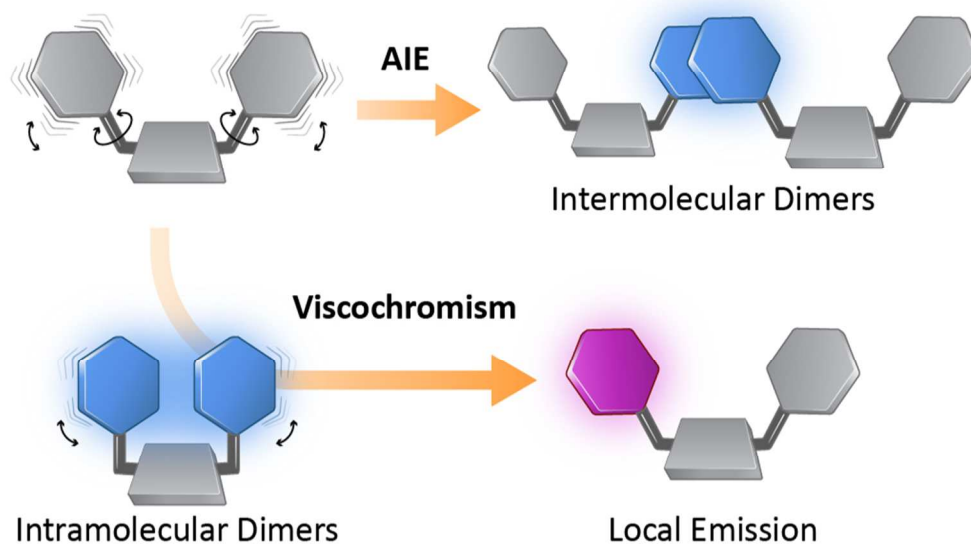


Figure 1. Schematic representation of the two processes that lead to face-to-face aromatic dimer formation, observed in the luminescence of the phenyl-ring molecular rotors. In the crystalline or aggregated states, enforced proximity of phenyl rings leads to emission from intermolecular aromatic dimers (shown in blue). A pair of interacting molecules is depicted, representing the local structure in an extended solid-state structure. In solution (i) the excitation may be lost through non-radiative decay, (ii) emission may arise from a relaxed state, brought about by intramolecular pairing (blue) of aromatic rings, or (iii) if dimer formation is prevented, a locally excited state decays by higher energy emission (purple).

177x102mm (150 x 150 DPI)

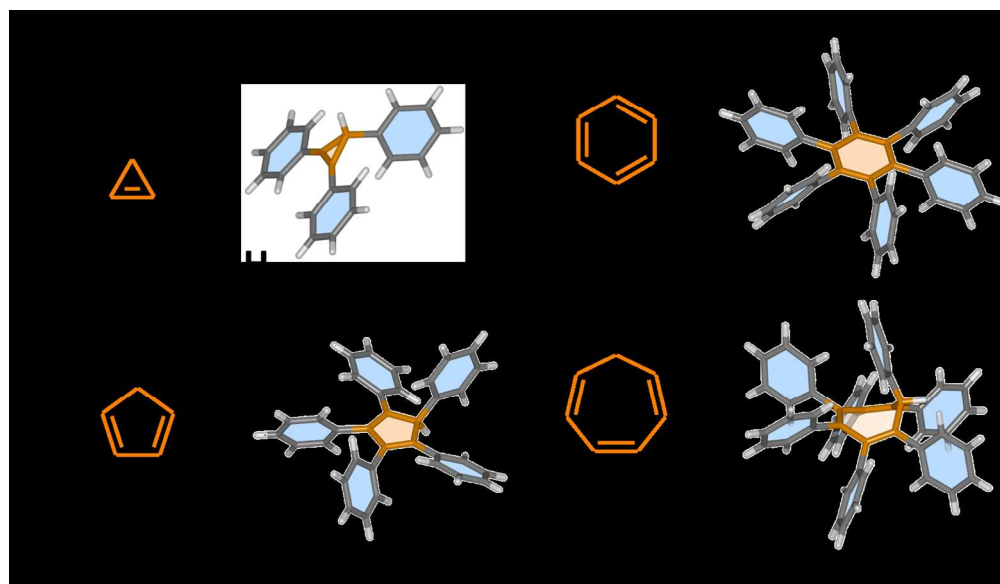


Figure 2. Structural formulas and X-ray crystal structures of (a) Ph<sub>3</sub>C<sub>3</sub>H, (b) Ph<sub>5</sub>C<sub>5</sub>H, (c) Ph<sub>6</sub>C<sub>6</sub>, and (d) Ph<sub>7</sub>C<sub>7</sub>H, showing the radial orientations of the peripheral phenyl rings around the central carbocycles (orange).

275x159mm (150 x 150 DPI)

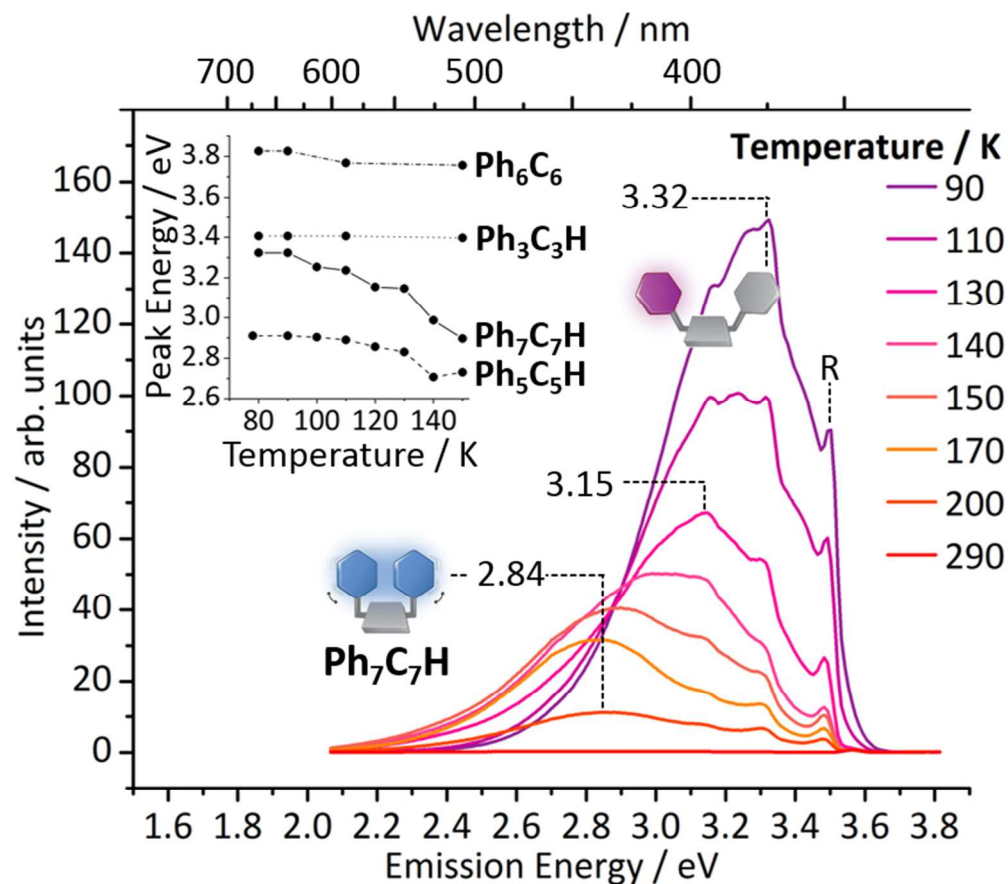


Figure 3. Steady-state photoluminescence spectroscopy of Ph<sub>7</sub>C<sub>7</sub>H (10  $\mu$ M solution in 2-MeTHF,  $E_{ex} = 3.94$  eV,  $l = 10$  mm) at a range of temperatures reveals luminescence from two different states. Inset: In contrast to Ph<sub>7</sub>C<sub>7</sub>H, the emission maxima of Ph<sub>3</sub>C<sub>3</sub>H and Ph<sub>6</sub>C<sub>6</sub> change very little as temperature is varied, whereas the emission from Ph<sub>5</sub>C<sub>5</sub>H undergoes a small hypsochromic shift at low temperature. The peak labeled 'R' is a result of Raman scattering from the solvent.<sup>17</sup>

144x126mm (150 x 150 DPI)

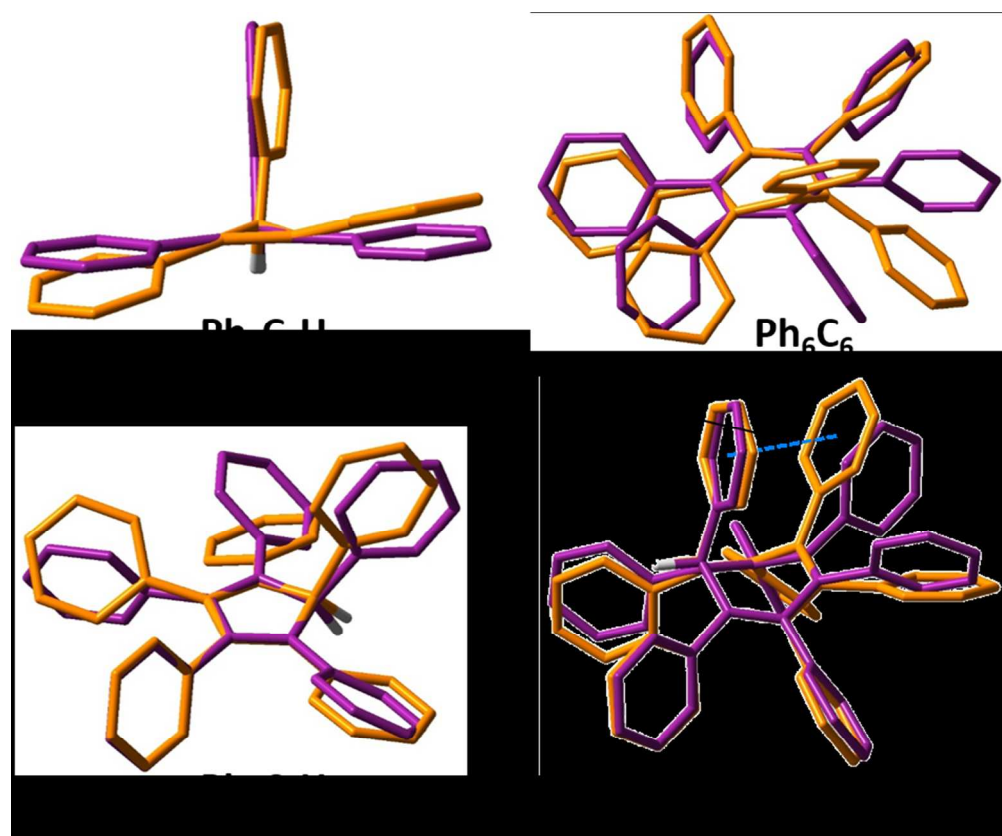


Figure 4. DFT minimum energy geometries calculated for the S<sub>0</sub> (purple) and S<sub>1</sub> (orange) electronic states of (a) Ph<sub>3</sub>C<sub>3</sub>H, (b) Ph<sub>5</sub>C<sub>5</sub>H, (c) Ph<sub>6</sub>C<sub>6</sub>, and (d) Ph<sub>7</sub>C<sub>7</sub>H, using the CAM-B3LYP22 functional, Def2-SVP basis set, and a C-PCM model to approximate PhMe as solvent. The dotted blue line illustrates a face-to-face interaction between distal phenyl rings of Ph<sub>7</sub>C<sub>7</sub>H in the S<sub>1</sub> state, characterized by a centroid-centroid distance of 3.89 Å and torsion angle of 22°. All H atoms at sp<sup>2</sup>-carbon centers are omitted for clarity.

161x133mm (150 x 150 DPI)

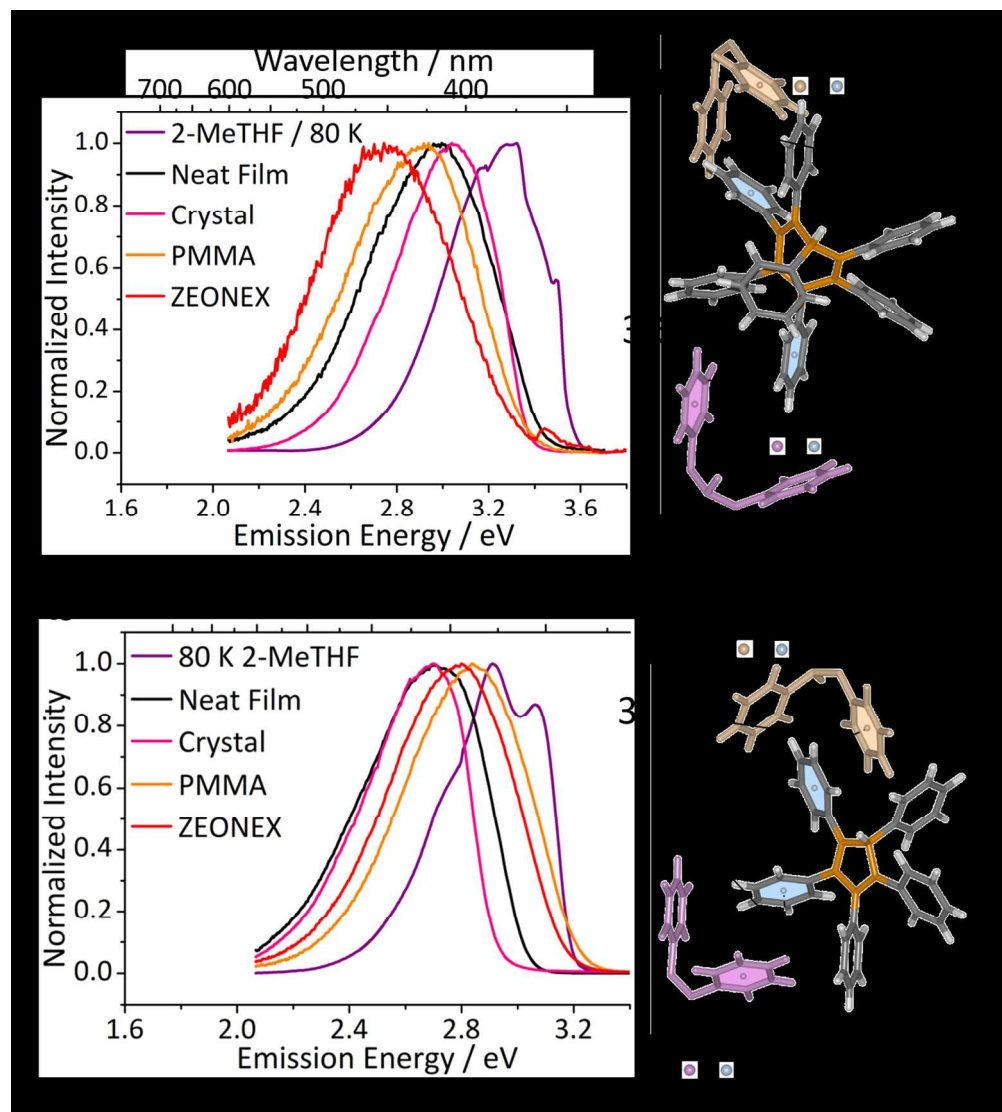


Figure 5. Emission profiles of (a) Ph7C7H and (b) Ph5C5H in crystalline and amorphous condensed phases are contrasted with the emission from frozen 2-MeTHF solutions. Solid-state packing interactions are shown for the carbocycles in (c) and (d), respectively. Colored spheres denote centroids and  $\varphi$  denotes the torsion angles between the planes defined by the atoms of the benzene rings.

236x261mm (150 x 150 DPI)

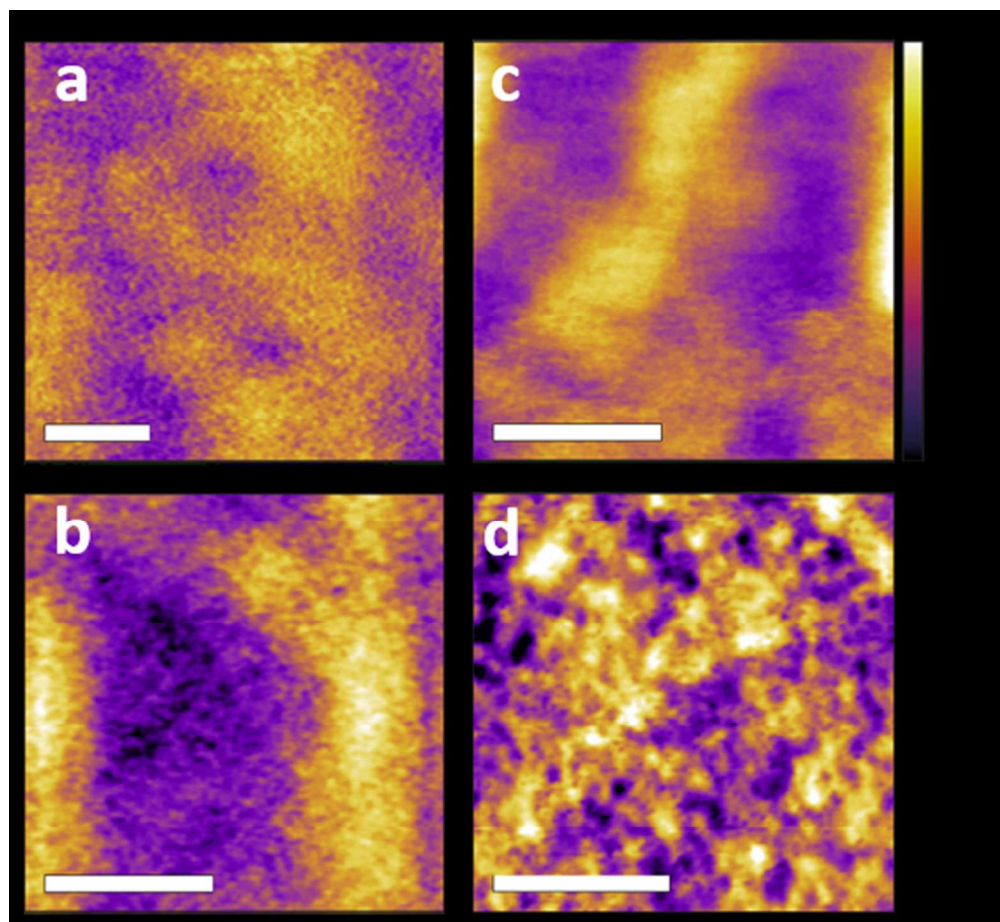


Figure 6. AFM images of spin-coated films of (a) Ph5C5H in PMMA, (b) Ph5C5H in ZEONEX®, (c) Ph7C7H in PMMA, and (d) Ph7C7H in ZEONEX®. Scale bars = 200 nm.

97x89mm (150 x 150 DPI)

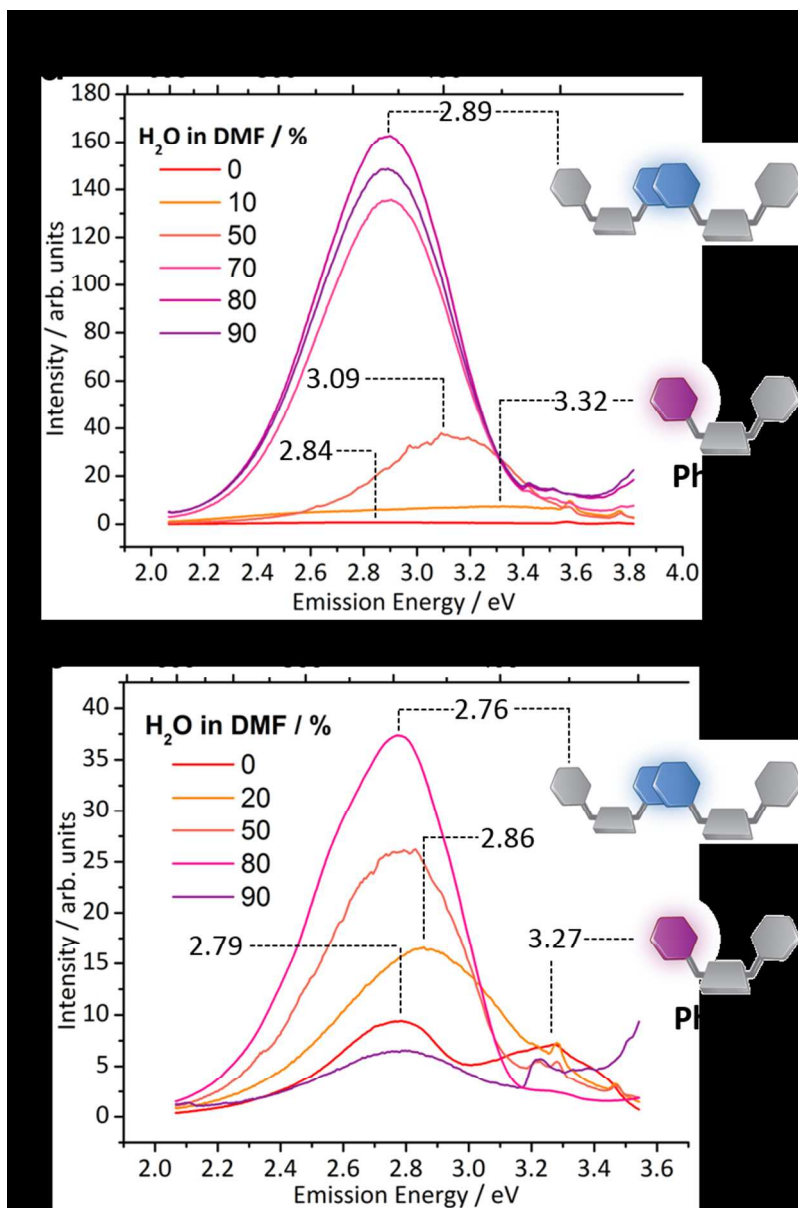


Figure 7. Steady-state photoluminescence spectra of (a) Ph7C7H and (b) Ph5C5H suspensions in H<sub>2</sub>O-DMF (E<sub>ex</sub> = 3.94 eV [Ph7C7H] / 3.65 eV [Ph5C5H], l = 10 mm, T = 298 K). As increasing proportions of H<sub>2</sub>O are added to the DMF solutions, emissive aggregates are formed. At high water contents, the emission energies are similar to the relaxed phenyl-dimer states observed in crystalline samples, which we ascribe to intermolecular interactions in the aggregates. Low intensity, higher energy emissions are observed from suspensions with lower water content (e.g., 10–50% for Ph7C7H), consistent with some localized emission. Small, sharp peaks above 3.20 eV in Figure 7b correspond to Raman scattering from the solvent.

145x218mm (150 x 150 DPI)

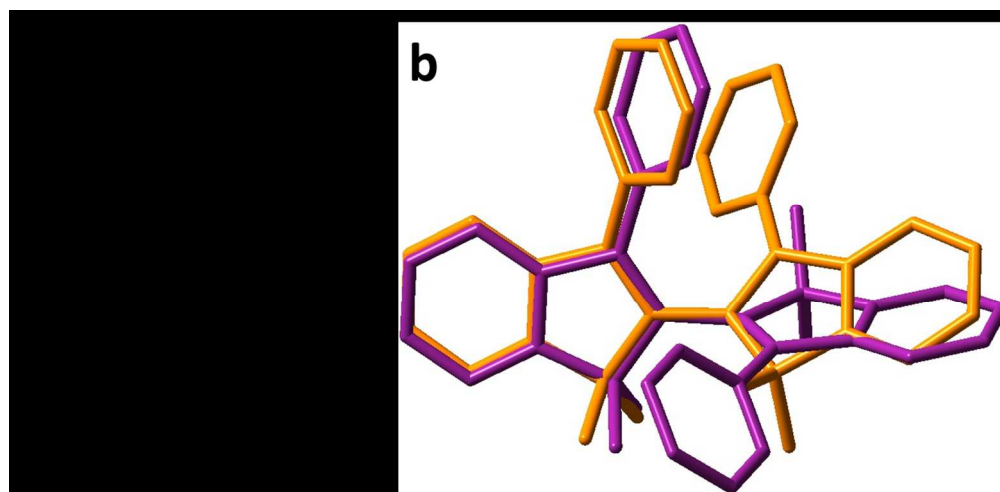


Figure 8. (a) Previously reported 2,2'-biindene 1 undergoes hypsochromic shift in its fluorescence upon aggregation. (b) Our DFT modelling of the S0 (purple) and S1 (orange) elec-tronic states suggests this effect results from a through-space aromatic dimer in solution, which cannot form in the aggre-gated-state. All H atoms are omitted for clarity.

249x121mm (150 x 150 DPI)

1  
2  
3  
4  
5  
6  
7  
8  
9  
10  
11  
12  
13  
14  
15  
16  
17  
18  
19  
20  
21  
22  
23  
24  
25  
26  
27  
28  
29  
30  
31  
32  
33  
34  
35  
36  
37  
38  
39  
40  
41  
42  
43  
44  
45  
46  
47  
48  
49  
50  
51  
52  
53  
54  
55  
56  
57  
58  
59  
60

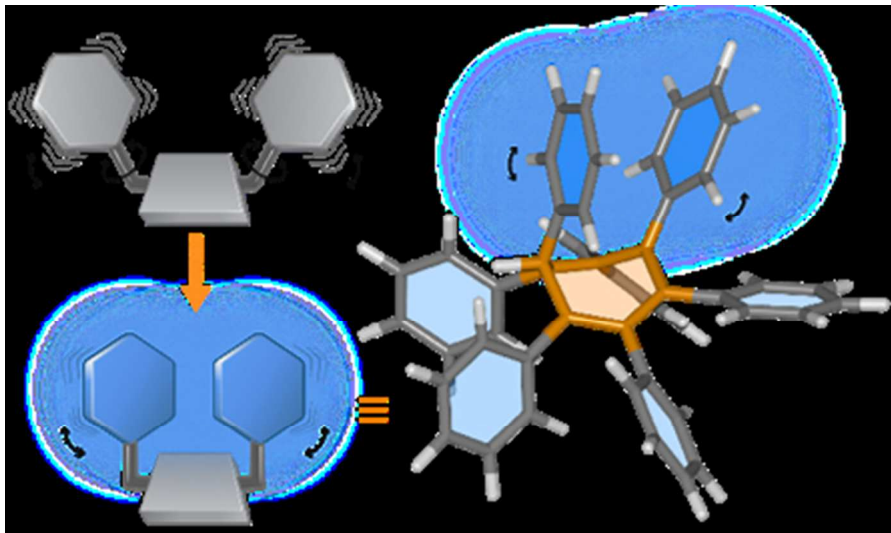


Table of Contents Graphic

75x44mm (150 x 150 DPI)